Hindawi
Mathematical Problems in Engineering
Volume 2018, Article ID 6123596, 16 pages
https://doi.org/10.1155/2018/6123596

Research Article

Analysis of Nonlinear Error Caused by Motions of Rotation Axes for Five-Axis Machine Tools with Orthogonal Configuration

Cong Geng,[1,2] **Yuhou Wu**,[1,2] **and Jian Qiu**[2,3]

[1]*National-Local Joint Engineering Laboratory of NC Machining Equipment and Technology of High-Grade Stone, Shenyang 110168, China*
[2]*School of Mechanical Engineering, Shenyang Jianzhu University, Shenyang 110168, China*
[3]*Shenyang Machine Tool (Group) Co., Ltd., Shenyang 110168, China*

Correspondence should be addressed to Cong Geng; 345886608@qq.com

Received 19 January 2018; Revised 8 April 2018; Accepted 8 May 2018; Published 28 June 2018

Academic Editor: Mohammed Nouari

Since a nonlinear relationship exists between the position coordinates of the rotation axes and components of the tool orientation, the tool will deviate from the required plane, resulting in nonlinear errors and deterioration of machining accuracy. Few attempts have been made to obtain a general formula and common rules for nonlinear error because of the existence of various kinematic structures of machine tools with orthogonal configuration. This paper analyzes the relationship between the deviation of cutter location points and motion of tool orientations. Five-axis CNC machine tools are divided into two groups according to the configuration of the two rotational joints and the home position. Motions of the tool are regarded as a combination of translation and rotation. A model for error calculation is then built. The maximum deviation of the tool with respect to the reference plane generated by the initial and the final orientation is used to quantify the magnitude of the errors. General formulas are derived and common change rules are analyzed. Finally, machining experiment is conducted to validate the theoretical analysis. The research has important implications on the selection of a particular kinematic configuration that may achieve higher accuracy for a specific machining task.

1. Introduction

Compared with the three-axis machine tool with three orthogonal translational axes, the five-axis machining center is equipped with two additional perpendicular rotational joints. The introduction of the two rotational joints makes it possible for machine tools to flexibly control its posture and gives full play for high-speed and high-efficiency machining of a wide range of complex work piece [1, 2], such as turbine blades, automotive, and aerospace parts.

The entire procedure for complex surface machining can be generally divided into the following steps. First, the CAM system uses curve segments to represent the surface generated by the CAD system. Next, the postprocessor turns the tool paths and tool orientations from machine independent to machine dependent format. Finally, the interpolation method is used to control the motions of three translational and two rotational joints during machining. The use of curve segments can significantly reduce the nonlinear error directly caused by the motion of translational axes [3]. However, since a nonlinear relationship exists between the position coordinates of the rotation axes and components of tool orientation, the tool will deviate from the plane generated by the initial and final tool orientations during machining and will travel in a curved trajectory instead of the desired straight path, leading to nonlinear error [4–7]. Therefore, research on the relationship between the motion of rotation axes and nonlinear errors has very important directive to improve machining efficiency and to achieve more accurate motion control of axes in five-axis machining.

A large variety of studies have investigated motions of rotation axes for different configurations of five-axis orthogonal machine tools from various perspectives. One category of such studies focused on kinematics analysis of the five-axis machine tools according to its structural configurations. Chen [8] found that there are 288 feasible configurations of

five-axis machining tools including machines with more or less than two rotational joints. Among them, machine tools equipped with two rotational joints are widely used in practice because this combination satisfies the best geometric and kinematic constraints. Efforts have been made to classify five-axis machine tools with three translational and two rotational joints, which are reciprocally orthogonal, into three basic types—rotary table (RT), spindle rotating (SR), and hybrid (HT)—according to the position of the two rotational joints, respectively [9–11]. Jung et al. [12] built a postprocessor that is suitable for the RT-type five-axis machine tool. Lee et al. [13] developed analytical equations capable of converting cutter location (CL) data and tool orientation vectors into machine control coordinates for the three representative types mentioned above. Several approaches have been proposed for building generic kinematic models that are applicable to all five-axis machine tool structures [14–19].

The other category of studies focused on nonlinear errors caused by the movement of the rotation axes. Hwang et al. [20] first observed that the structure of NC machines should be taken into consideration for error estimation in five-axis CNC machining. Similarly, Srijuntongsiri et al. [21] pointed out that the difference between the actual and the desired trajectories in five-axis machining depends only on the configuration of the machine, provided that the tool path is fixed. Jun et al. [22] found that the surface error is related to the variation of the tool orientation. Sencer et al. [23] then built a kinematic model to estimate the error during five-axis motion. Although the papers mentioned above acknowledged that nonlinear errors in five-axis machining should focus on the configuration of machine tools and the variation of tool orientation, minimal attempts have been made to quantify their magnitude. To address this problem, a method was proposed [24] to evaluate the nonlinear errors induced by the motion of the rotary axes of vertical SR five-axis machine tools. Yang et al. [25] analyzed nonlinear errors introduced by the motion of the rotation axes under the condition that the tool can rotate about the Z-axis and Y-axis, and the initial orientation is parallel to the Z-axis. Geng et al. [26, 27] studied tool movement procedure of AB spindle rotating machine tool and AC rotary table machine tool and predicted nonlinear errors due to the movement of the rotation axes. However, the models discussed above are only suitable for one specific machine type, which is not comprehensive. A general model and common rules for nonlinear errors due to the motions of the rotation axes of five-axis machine tools with orthogonal configuration are still lacking.

Therefore, the present study will thoroughly analyze nonlinear errors due to the motions of the rotation axes of different configuration structures of machine tools. A general model of nonlinear errors due to the movement of the rotation axes will be developed. The remainder of this paper is organized as follows. In Section 2, kinematic structures of five-axis orthogonal CNC machine tools with three linear axes and two rotation axes are discussed. A classification method is proposed to divide machine tools into two groups according to the configuration of two rotational joints and the home position of tool orientation. A model for estimating nonlinear errors due to the motions of the rotation axes is built and the formula is discussed in Section 3. In Section 4, formulas of nonlinear errors due to the movement of the rotation axes are derived based on the proposed model, and common rules are analyzed for machine tools in both groups. Details of experiments are presented in Section 5 and conclusions from the study are made in Section 6.

2. Classification of Five-Axis Machine Tools

Theoretically, a five-axis machine tool can have a random placement of the five translational and rotational joints from X, Y, Z, A, B, and C. According to this theory, 288 different configurations [4] can be found. However, since machine tools with more or less than two rotary axes have little industrial application, these types of machine tools will not be considered in this paper. In this section, we will investigate machine tools with three linear axes X, Y, and Z and two of the three rotation axes A, B, and C that, respectively, rotate about the X-, Y-, and Z-axis. For five-axis machine tools with two rotation axes, one criterion that was proposed early and has been widely used for categorization is based on the position of the two rotational joints [14]. According to this criterion, five-axis machine tools can be grouped into three types—spindle rotating(SR) type, rotary table(RT) type, and hybrid(HT) type. The SR type machine tools refer to those whose rotation axes are both placed on the spindle. The RT-type machine tools refer to those whose rotation axes are both placed on the workpiece. Those with one rotary placed on the workpiece and the other placed on the spindle side are classified as the hybrid type.

For the SR type and the RT type, of the two rotation axes, the one which is placed closer than the other to the machine bed within the kinematic chain is called the primary rotation axis. The other rotation axis is referred to as the secondary axis. In machining, the primary rotation axis has a fixed spatial direction, while the secondary axis moves, and the position of the secondary axis varies with the motion of the primary rotation axis. Therefore, for the RT-type machine, the relationship between the tool orientation V_i in WCS (work coordinate system) and rotation angles in MCS(machine coordinate system) can be expressed as [13]

$$V_i = R_{PS}\left(\theta_{PS,i}\right) \cdot R_{SS}\left(\theta_{SS,i}\right) \cdot p^T, \tag{1}$$

where p^T is the home position of tool orientation corresponding to the position where both rotation angles are equal to zero and is usually set to be parallel to one of the machine translational axes, and $R_{PS}(\theta_{PS,i})$ and $R_{SS}(\theta_{SS,i})$ are rotational matrixes of the primary spindle rotation and the secondary spindle rotation whose rotational angles are, respectively, specified by $\theta_{PS,i}$ and $\theta_{SS,i}$. Similarly, for the SR type machine, the coordinate transformation equation can be written as [13]

$$V_i = R_{ST}\left(\theta_{ST,i}\right) \cdot R_{PT}\left(\theta_{PT,i}\right) \cdot p^T, \tag{2}$$

where $R_{ST}(\theta_{ST,i})$ and $R_{PT}(\theta_{PT,i})$ are rotational matrixes of the secondary table rotation and the primary table rotation whose rotational angles are, respectively, specified by $\theta_{ST,i}$

and $\theta_{PT,i}$. For the HT type machine, both axes are called the primary rotation axes, since the positions of the rotation axes do not change with each other. In machining, the following equation exists [13]:

$$V_i = R_{PT}\left(\theta_{PT,i}\right) \cdot R_{PS}\left(\theta_{PS,i}\right) \cdot p^T. \tag{3}$$

The coordinate transformation equations expressed in (1), (2), and (3) can further be modified to a more generic form in which the tool orientation V_i in WCS can be obtained after rotating the home position of the tool orientation p^T by $\theta_{m,i}$, first around the m-axis, and by $\theta_{k,i}$ around the k-axis successively [15]:

$$V_i = R_k\left(\theta_{k,i}\right) \cdot R_m\left(\theta_{m,i}\right) \cdot p^T \quad k, m \in \{X, Y, Z\}, \tag{4}$$

where $R_k(\theta_{k,i})$ and $R_m(\theta_{m,i})$ can be determined by one of the following three representation forms depending on its rotation axes:

$$R_X\left(\theta_{X,i}\right) = \begin{bmatrix} 1 & 0 & 0 \\ 0 & \cos\theta_{X,i} & -\sin\theta_{X,i} \\ 0 & \sin\theta_{X,i} & \cos\theta_{X,i} \end{bmatrix}, \tag{5}$$

$$R_Y\left(\theta_{Y,i}\right) = \begin{bmatrix} \cos\theta_{Y,i} & 0 & \sin\theta_{Y,i} \\ 0 & 1 & 0 \\ -\sin\theta_{Y,i} & 0 & \cos\theta_{Y,i} \end{bmatrix}, \tag{6}$$

$$R_z\left(\theta_{Z,i}\right) = \begin{bmatrix} \cos\theta_{Z,i} & -\sin\theta_{Z,i} & 0 \\ \sin\theta_{Z,i} & \cos\theta_{Z,i} & 0 \\ 0 & 0 & 1 \end{bmatrix}. \tag{7}$$

From the above-mentioned procedure, it can be observed that the motion of the tool during machining is influenced by the configuration of two rotational joints and the home position, and not the machine type. Therefore, in this paper, five-axis machine tools will be classified according to their rotary axis features and home position. The rotary axis features consist of two characters-AB, AC, BC, BA, CA, and CB-, which are in the order of the work coordinate system to the tool coordinate system (TCS). The home position of the tool orientation cannot be parallel to the rotation axis specified by the second character, since it is not feasible for a tool to rotate about its own axis, which means that each type of rotary axis feature has two appropriate cutter orientations to enable five-axis machining. Therefore, five-axis machine tools can be recognized as the following twelve types presented in Table 1. The types of machine tools are specified by three characters in which the first two characters determine the rotary axis feature and the last character refers to the home position. Those whose home positions are parallel to the rotation axis specified by the first character are grouped into Group I, while others are in Group II.

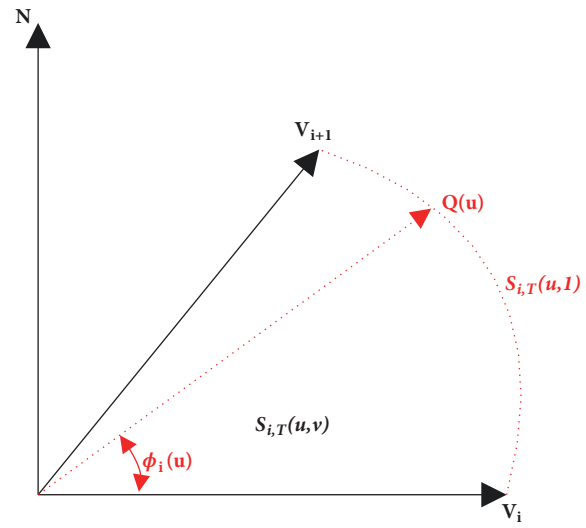

FIGURE 1: Schematic diagram of plain $S_{i,T}(u, v)$.

3. Definition of Nonlinear Error due to Motions of Rotary Axes

As shown in (4), for the tool whose home position $\boldsymbol{p}$ moves from $\boldsymbol{V_i}$ to $\boldsymbol{V_{i+1}}$, the two rotations will change, respectively, from $\theta_{k,i}$ and $\theta_{m,i}$ to $\theta_{k,i+1}$ and $\theta_{m,i+1}$:

$$\begin{aligned} V_i &= R_k\left(\theta_{k,i}\right) \cdot R_m\left(\theta_{m,i}\right) \cdot p^T \\ V_{i+1} &= R_k\left(\theta_{k,i+1}\right) \cdot R_m\left(\theta_{m,i+1}\right) \cdot p^T. \end{aligned} \tag{8}$$

The corresponding surface $S_{i,R}(u, v)$ that is defined by tool orientations in machining can be expressed as

$$\begin{aligned} S_{i,R}(u, v) &= v \cdot P(u) \\ P(u) &= R_k\left(\theta_{k,i}(u)\right) \cdot R_m\left(\theta_{m,i}(u)\right) \cdot p^T, \end{aligned} \tag{9}$$

where u and v are parameters changed from 0 to 1. $\theta_{k,i}(u)$ and $\theta_{m,i}(u)$ are affected by the type of interpolation used to decide intermediate tool orientations along the tool path. In five-axis machining, linear interpolation and tool orientation interpolation are the two functions that are commonly employed by the CNC system. Tool orientation interpolation can lead to vibration of machine tool in singular areas; therefore, linear interpolation of rotation axes is preferred in machining. In the following analysis, the linear interpolation method is used as an example and similar analyses can be carried out for tool orientation interpolation:

$$\begin{aligned} \theta_{k,i}(u) &= (1-u)\,\theta_{k,i} + u\theta_{k,i+1} \\ \theta_{m,i}(u) &= (1-u)\,\theta_{m,i} + u\theta_{m,i+1}. \end{aligned} \tag{10}$$

The plane $S_{i,T}(u, v)$ determined by V_i and V_{i+1} can be expressed as follows:

$$S_{i,T}(u, v) = v \cdot Q(u) \tag{11}$$

where u and v are parameters changing from 0 to 1. As shown in Figure 1, the point Q(u) is on the curve

Table 1: Classification of five-axis machine tools according to configuration of rotation axes.

Group	Type	Rotary axis features	Home position	Tool orientation
I	ABX	AB	$(1\ 0\ 0)$	$\begin{pmatrix} \cos\theta_{Y,i} \\ \sin\theta_{X,i}\cdot\sin\theta_{Y,i} \\ -\cos\theta_{X,i}\cdot\sin\theta_{Y,i} \end{pmatrix}$
	ACX	AC	$(1\ 0\ 0)$	$\begin{pmatrix} \cos\theta_{Z,i} \\ \cos\theta_{X,i}\cdot\sin\theta_{Z,i} \\ \sin\theta_{X,i}\cdot\sin\theta_{Z,i} \end{pmatrix}$
	BCY	BC	$(0\ 1\ 0)$	$\begin{pmatrix} -\cos\theta_{Y,i}\cdot\sin\theta_{Z,i} \\ \cos\theta_{Z,i} \\ \sin\theta_{Y,i}\cdot\sin\theta_{Z,i} \end{pmatrix}$
	BAY	BA	$(0\ 1\ 0)$	$\begin{pmatrix} \sin\theta_{X,i}\cdot\sin\theta_{Y,i} \\ \cos\theta_{X,i} \\ \sin\theta_{X,i}\cdot\cos\theta_{Y,i} \end{pmatrix}$
	CAZ	CA	$(0\ 0\ 1)$	$\begin{pmatrix} \sin\theta_{X,i}\cdot\sin\theta_{Z,i} \\ -\sin\theta_{X,i}\cdot\cos\theta_{Z,i} \\ \cos\theta_{X,i} \end{pmatrix}$
	CBZ	CB	$(0\ 0\ 1)$	$\begin{pmatrix} \sin\theta_{Y,i}\cdot\cos\theta_{Z,i} \\ \sin\theta_{Y,i}\cdot\sin\theta_{Z,i} \\ \cos\theta_{Y,i} \end{pmatrix}$
II	ABZ	AB	$(0\ 0\ 1)$	$\begin{pmatrix} \sin\theta_{Y,i} \\ -\sin\theta_{X,i}\cdot\cos\theta_{Y,i} \\ \cos\theta_{X,i}\cdot\cos\theta_{Y,i} \end{pmatrix}$
	ACY	AC	$(0\ 1\ 0)$	$\begin{pmatrix} -\sin\theta_{Z,i} \\ \cos\theta_{X,i}\cdot\cos\theta_{Z,i} \\ \sin\theta_{X,i}\cdot\cos\theta_{Z,i} \end{pmatrix}$
	BCX	BC	$(1\ 0\ 0)$	$\begin{pmatrix} \cos\theta_{Y,i}\cdot\cos\theta_{Z,i} \\ \sin\theta_{Z,i} \\ -\sin\theta_{Y,i}\cdot\cos\theta_{Z,i} \end{pmatrix}$
	BAZ	BA	$(0\ 0\ 1)$	$\begin{pmatrix} \cos\theta_{X,i}\cdot\sin\theta_{Y,i} \\ -\sin\theta_{X,i} \\ \cos\theta_{X,i}\cdot\cos\theta_{Y,i} \end{pmatrix}$
	CAY	CA	$(0\ 1\ 0)$	$\begin{pmatrix} -\cos\theta_{X,i}\cdot\sin\theta_{Z,i} \\ \cos\theta_{X,i}\cdot\cos\theta_{Z,i} \\ \sin\theta_{X,i} \end{pmatrix}$
	CBX	CB	$(1\ 0\ 0)$	$\begin{pmatrix} \cos\theta_{Y,i}\cdot\cos\theta_{Z,i} \\ \sin\theta_{Z,i}\cdot\cos\theta_{Y,i} \\ -\sin\theta_{Y,i} \end{pmatrix}$

$S_{i,T}(u, 1)$ and $\phi_i(u)$ is the angle between the vector Q(u) and V_i:

$$Q(u) = \cos\phi_i(u)\,\boldsymbol{V}_i + \sin\phi_i(u)\,N \tag{12}$$

As parameter u varies from 0 to 1, the vector Q(u) moves from V_i to V_{i+1} and $\phi_i(u)$ can be expressed by the following function:

$$\phi_i(u) = \arccos\left(\frac{\boldsymbol{V}_i\cdot\boldsymbol{V}_{i+1}}{\|\mathbf{V}_i\|\cdot\|\mathbf{V}_{i+1}\|}\right)\cdot u \tag{13}$$

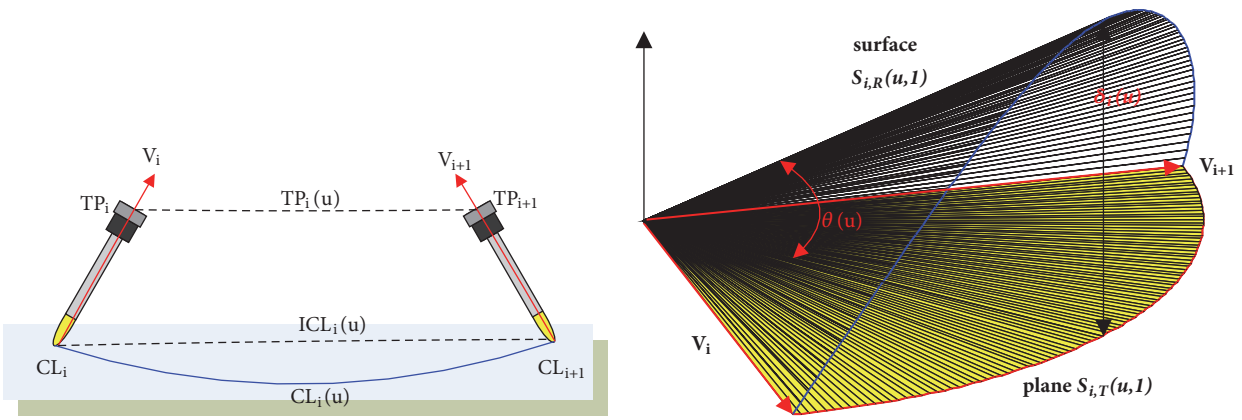

(a) Cutter motion (b) Tool orientation deviation

FIGURE 2: Schematic diagram of nonlinear error.

N is a unit vector who lies on plane $S_{i,T}(u,v)$ and is perpendicular to V_i. Under the condition that u = 1, Q(u) arrive at the position V_{i+1},

$$V_{i+1} = \cos\phi_i(1)\,\mathbf{V}_i + \sin\phi_i(1)\,N \tag{14}$$

Therefore, N satisfies the following equation:

$$N = \frac{V_{i+1} - \cos\phi_i(1)\,V_i}{\sin\phi_i(1)} \tag{15}$$

Equation (11) can therefore be transformed as

$$\begin{aligned} S_{i,T}(u,v) &= v \cdot Q(u) \\ Q(u) &= \left(\cos\phi_i(u) - \frac{\cos\phi_i(1)}{\sin\phi_i(1)}\sin\phi_i(u)\right)\boldsymbol{V}_i \\ &\quad + \frac{\sin\phi_i(u)}{\sin\phi_i(1)}\boldsymbol{V}_{i+1} \end{aligned} \tag{16}$$

The tool will move on the surface $S_{i,R}(u,v)$ instead of the ideal plane $S_{i,T}(u,v)$ passing through the start and the end orientation vectors owing to the nonlinear relationship between tool orientation vectors and rotation axes, as shown in (9). As shown in Figure 2(a), movements of the tool are generally defined by straight-line motions of the machine's pivot point. Thus, while the machine's pivot point follows a linear trajectory $TP_i(u)$ from TP_i to TP_{i+1}, the ideal cutter location point can be expressed as [24]

$$ICL_i(u) = (1-u)\,TP_i + uTP_{i+1} - LQ(u), \tag{17}$$

where L is the tool length. The actual cutter location point will be on the nonlinear trajectory $CL_i(u)$, since $S_{i,R}(u,v)$ and $S_{i,T}(u,v)$ are different:

$$CL_i(u) = (1-u)\,TP_i + uTP_{i+1} - LP(u). \tag{18}$$

The distance $\delta_i(u)$ between $CL_i(u)$ and $ICL_i(u)$ can be derived by

$$\begin{aligned} \delta_i(u) &= \left|CC_i(u) - ICC_i(u)\right| = L\alpha_{i,u} \\ \alpha_{i,u} &= \left|Q(u) - P(u)\right| = \sqrt{2\left(1-\cos\theta(u)\right)} \\ &\approx \sin\theta(u), \end{aligned} \tag{19}$$

where $\theta(u)$ specifies the angle between the two unit vectors Q(u) and P(u) and satisfies the following equation:

$$\sin\theta(u) = S_{i,R}(u,1)\cdot\left(S_{i,T}(0,1)\times S_{i,T}(1,1)\right). \tag{20}$$

As shown in Figure 2(b), the nonlinear error δ_i is defined as the maximum value of $\delta_i(u)$:

$$\begin{aligned} \delta_i = \Big\{ &\max_{u\in[0,1]}\left(\delta_i(u)\right) \mid \delta_i(u) = L\cdot S_{i,R}(u,1) \\ &\cdot\left(S_{i,T}(0,1)\times S_{i,T}(1,1)\right)\Big\}. \end{aligned} \tag{21}$$

4. Analysis of Nonlinear Error due to Movement of Rotation Axes

As mentioned above, previous studies have focused mainly on nonlinear error due to the motions of the rotation axes for one specific machine type. The general formula and common rules for five-axis machine tools with orthogonal configuration have rarely been mentioned. In this section, based on the calculation equation of nonlinear error proposed in Section 3, nonlinear errors due to the rotational movement for five-axis machine tools with various configurations presented in Table 1 are analyzed and common rules for machines in Group I and Group II are then analyzed, respectively.

4.1. General Formula and Common Rules of Nonlinear Error due to Rotational Movement for Machine Tools in Group I. As presented in Table 2, $\alpha_{i,u}$ can be obtained according to (19) for five-axis machine tools with various configurations listed in Group I. The detailed calculation procedure for the machine tool of type ABX is presented as an example in Appendix A, which can be extended to the other types in Group I.

Table 2: Detailed expressions of $\alpha_{i,u}$ for machine tool in Group I.

Type	Deviation of $S_{i,R}(u,1)$ from the reference plane $S_{i,T}(u,1)$
ABX	$\left\lvert \dfrac{\sin(\theta_{Y,i})\sin(\theta_{Y,i+1})\cos((1-u)\theta_{Y,i}+u\theta_{Y,i+1})\sin(\theta_{X,i+1}-\theta_{X,i}) - \sin((1-u)\theta_{Y,i}+u\theta_{Y,i+1})\sin(\theta_{Y,i+1})\cos(\theta_{Y,i})\sin((1-u)(\theta_{X,i+1}-\theta_{X,i})) - \sin((1-u)\theta_{Y,i}+u\theta_{Y,i+1})\cos(\theta_{Y,i+1})\sin(\theta_{Y,i})\sin(u(\theta_{X,i+1}-\theta_{X,i}))}{\sqrt{1-(\cos(\theta_{Y,i})\cos(\theta_{Y,i+1})+\sin(\theta_{Y,i})\sin(\theta_{Y,i+1})\cos(\theta_{X,i+1}-\theta_{X,i}))^2}} \right\rvert$
ACX	$\left\lvert \dfrac{\sin(\theta_{Z,i})\sin(\theta_{Z,i+1})\cos((1-u)\theta_{Z,i}+u\theta_{Z,i+1})\sin(\theta_{X,i+1}-\theta_{X,i}) - \sin((1-u)\theta_{Z,i}+u\theta_{Z,i+1})\sin(\theta_{Z,i+1})\cos(\theta_{Z,i})\sin((1-u)(\theta_{X,i+1}-\theta_{X,i})) - \sin((1-u)\theta_{Z,i}+u\theta_{Z,i+1})\cos(\theta_{Z,i+1})\sin(\theta_{Z,i})\sin(u(\theta_{X,i+1}-\theta_{X,i}))}{\sqrt{1-(\cos(\theta_{Z,i})\cos(\theta_{Z,i+1})+\sin(\theta_{Z,i})\sin(\theta_{Z,i+1})\cos(\theta_{X,i+1}-\theta_{X,i}))^2}} \right\rvert$
BCY	$\left\lvert \dfrac{\sin(\theta_{Z,i})\sin(\theta_{Z,i+1})\cos((1-u)\theta_{Z,i}+u\theta_{Z,i+1})\sin(\theta_{Y,i+1}-\theta_{Y,i}) - \sin((1-u)\theta_{Z,i}+u\theta_{Z,i+1})\sin(\theta_{Z,i+1})\cos(\theta_{Z,i})\sin((1-u)(\theta_{Y,i+1}-\theta_{Y,i})) - \sin((1-u)\theta_{Z,i}+u\theta_{Z,i+1})\cos(\theta_{Z,i+1})\sin(\theta_{Z,i})\sin(u(\theta_{Y,i+1}-\theta_{Y,i}))}{\sqrt{1-(\cos(\theta_{Z,i})\cos(\theta_{Z,i+1})+\sin(\theta_{Z,i})\sin(\theta_{Z,i+1})\cos(\theta_{Y,i+1}-\theta_{Y,i}))^2}} \right\rvert$
BAY	$\left\lvert \dfrac{\sin(\theta_{X,i})\sin(\theta_{X,i+1})\cos((1-u)\theta_{X,i}+u\theta_{X,i+1})\sin(\theta_{Y,i+1}-\theta_{Y,i}) - \sin((1-u)\theta_{X,i}+u\theta_{X,i+1})\sin(\theta_{X,i+1})\cos(\theta_{X,i})\sin((1-u)(\theta_{Y,i+1}-\theta_{Y,i})) - \sin((1-u)\theta_{X,i}+u\theta_{X,i+1})\cos(\theta_{X,i+1})\sin(\theta_{X,i})\sin(u(\theta_{Y,i+1}-\theta_{Y,i}))}{\sqrt{1-(\cos(\theta_{X,i})\cos(\theta_{X,i+1})+\sin(\theta_{X,i})\sin(\theta_{X,i+1})\cos(\theta_{Y,i+1}-\theta_{Y,i}))^2}} \right\rvert$
CAZ	$\left\lvert \dfrac{\sin(\theta_{X,i})\sin(\theta_{X,i+1})\cos((1-u)\theta_{X,i}+u\theta_{X,i+1})\sin(\theta_{Z,i+1}-\theta_{Z,i}) - \sin((1-u)\theta_{X,i}+u\theta_{X,i+1})\sin(\theta_{X,i+1})\cos(\theta_{X,i})\sin((1-u)(\theta_{Z,i+1}-\theta_{Z,i})) - \sin((1-u)\theta_{X,i}+u\theta_{X,i+1})\cos(\theta_{X,i+1})\sin(\theta_{X,i})\sin(u(\theta_{Z,i+1}-\theta_{Z,i}))}{\sqrt{1-(\cos(\theta_{X,i})\cos(\theta_{X,i+1})+\sin(\theta_{X,i})\sin(\theta_{X,i+1})\cos(\theta_{Z,i+1}-\theta_{Z,i}))^2}} \right\rvert$
CBZ	$\left\lvert \dfrac{\sin(\theta_{Y,i})\sin(\theta_{Y,i+1})\cos((1-u)\theta_{Y,i}+u\theta_{Y,i+1})\sin(\theta_{Z,i+1}-\theta_{Z,i}) - \sin((1-u)\theta_{Y,i}+u\theta_{Y,i+1})\sin(\theta_{Y,i+1})\cos(\theta_{Y,i})\sin((1-u)(\theta_{Z,i+1}-\theta_{Z,i})) - \sin((1-u)\theta_{Y,i}+u\theta_{Y,i+1})\cos(\theta_{Y,i+1})\sin(\theta_{Y,i})\sin(u(\theta_{Z,i+1}-\theta_{Z,i}))}{\sqrt{1-(\cos(\theta_{Y,i})\cos(\theta_{Y,i+1})+\sin(\theta_{Y,i})\sin(\theta_{Y,i+1})\cos(\theta_{Z,i+1}-\theta_{Z,i}))^2}} \right\rvert$

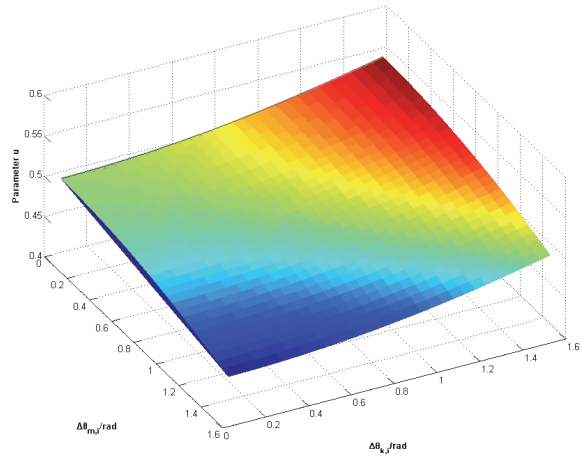

FIGURE 3: Parameter u corresponding to maximum $\alpha_{i,u}$ for machine tools in Group I.

Assuming that the tool orientation changes from V_i to V_{i+1} and that the two rotary axes move, respectively, from $\theta_{k,i}$ and $\theta_{m,i}$ to $\theta_{k,i+1}$ and $\theta_{m,i+1}$, it can be concluded from Table 2 that the deviation of $S_{i,R}(u, 1)$ from the reference plane $S_{i,T}(u, 1)$ for machine tools in Group I can be calculated according to the following equation:

$$\alpha_{i,u} = \left| \frac{\sin(\theta_{m,i}) \sin(\theta_{m,i+1}) \cos((1-u)\theta_{m,i} + u\theta_{m,i+1}) \sin(\theta_{k,i+1} - \theta_{k,i}) - \sin((1-u)\theta_{m,i} + u\theta_{m,i+1}) \sin(\theta_{m,i+1}) \cos(\theta_{m,i}) \sin((1-u)(\theta_{k,i+1} - \theta_{k,i})) - \sin((1-u)\theta_{m,i} + u\theta_{m,i+1}) \cos(\theta_{m,i+1}) \sin(\theta_{m,i}) \sin(u(\theta_{k,i+1} - \theta_{k,i}))}{\sqrt{1 - (\cos(\theta_{m,i}) \cos(\theta_{m,i} + \Delta\theta_{m,i}) + \sin(\theta_{m,i}) \sin(\theta_{m,i} + \Delta\theta_{m,i}) \cos(\Delta\theta_{k,i}))^2}} \right| \quad (22)$$

where $\Delta\theta_{k,i}$ and $\Delta\theta_{m,i}$ are incremental values for the two rotation axes given by

$$\begin{aligned} \Delta\theta_{k,i} &= \theta_{k,i+1} - \theta_{k,i} \\ \Delta\theta_{m,i} &= \theta_{m,i+1} - \theta_{m,i}. \end{aligned} \quad (23)$$

The determination of δ_i is actually a maximization problem of $\alpha_{i,u}$ with u as the variable, which means that the solutions will be found under the following condition:

$$\frac{d\delta_i(u)}{du} = L\frac{d\alpha_{i,u}}{du} = 0. \quad (24)$$

Since transcendental equations exist in the problem solving procedure, it is difficult to find an analytical solution to (24). As is depicted in Figure 3, numerical solutions to calculating parameter u that can satisfy (24) under the condition that $\Delta\theta_{k,i}$ and $\Delta\theta_{m,i}$ vary from 0 to pi/2 are obtained. According to this figure, the maximum $\alpha_{i,u}$ can be observed with parameter u varying from 0.4535 to 0.5465 for machine tools in Group I. Therefore, to simplify the calculation, δ_{Ii} can be regarded as the approximate value of $\alpha_{i,u}$ when u is equal to 0.5:

$$\begin{aligned} &\delta_{Ii}(\theta_{m,i}, \Delta\theta_{m,i}, \Delta\theta_{k,i}) \\ &\approx \left| \frac{\sin(\theta_{m,i}) \sin(\theta_{m,i} + \Delta\theta_{m,i}) \cos(\theta_{m,i} + (1/2)\Delta\theta_{m,i}) \sin(\Delta\theta_{k,i}) - \sin(\theta_{m,i} + (1/2)\Delta\theta_{m,i}) \sin((1/2)\Delta\theta_{k,i}) \sin(2\theta_{m,i} + \Delta\theta_{m,i})}{\sqrt{1 - (\cos(\theta_{m,i}) \cos(\theta_{m,i} + \Delta\theta_{m,i}) + \sin(\theta_{m,i}) \sin(\theta_{m,i} + \Delta\theta_{m,i}) \cos(\Delta\theta_{k,i}))^2}} \right| \end{aligned} \quad (25)$$

Regarding (25), some important observations can be made.

(1) Nonlinear error can be represented as a function of $\theta_{m,i}$, $\Delta\theta_{k,i}$, and $\Delta\theta_{m,i}$. The variation of the nonlinear error is independent of the rotational angle $\theta_{k,i}$. As is shown in Figure 4, under the conditions that $\Delta\theta_{k,i} = 30^\circ$, $\Delta\theta_{m,i} = 15^\circ$, and $\theta_{m,i} = 10^\circ$, the nonlinear error is constant when $\theta_{k,i}$ varies from -180° to 180°.

(2) Under the condition that $\theta_{m,i} = 0$, the nonlinear error δ_{Ii} can be simplified into a function which is merely related to the incremental values of the rotation axes $\Delta\theta_{k,i}$ and $\theta_{m,i}$:

$$\begin{aligned} &\delta_{Ii}(\theta_{m,i}, \Delta\theta_{m,i}, \Delta\theta_{k,i})\big|_{\theta_{m,i}=0} \\ &= \left| \sin\left(\frac{1}{2}\Delta\theta_{m,i}\right) \sin\left(\frac{1}{2}\Delta\theta_{k,i}\right) \right| \approx \left| \frac{1}{4}\Delta\theta_{k,i}\Delta\theta_{m,i} \right|. \end{aligned} \quad (26)$$

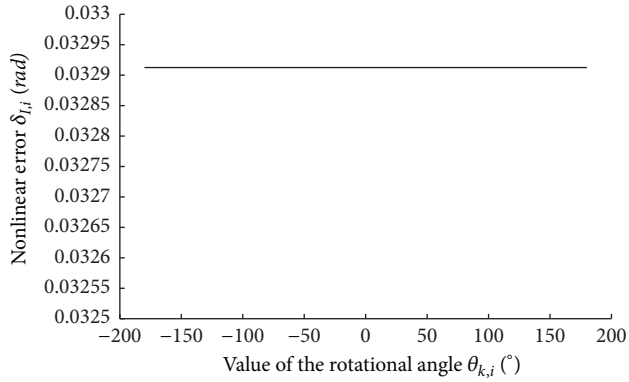

FIGURE 4: Influence of $\theta_{k,i}$ on nonlinear error δ_{Ii}.

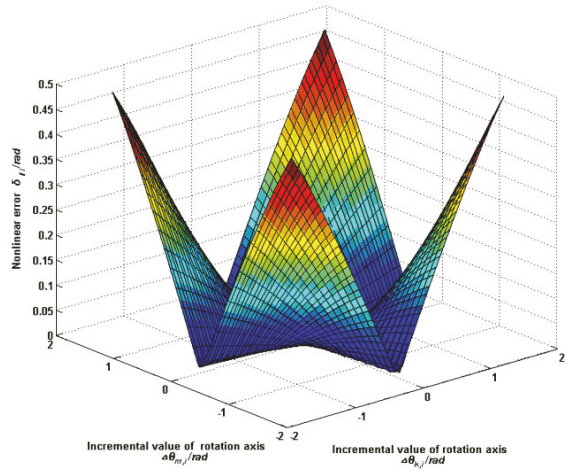

FIGURE 5: Nonlinear error curve under the condition that $\theta_{m,i} = 0$.

According to (26), the nonlinear errors δ_{Ii} are zero under the condition that there is only one rotation axis involved in machining. Figure 5 depicts the corresponding nonlinear error curve when $\theta_{m,i}$ is set to zero and incremental values for the two rotation axes vary from $-\pi/2$ to $\pi/2$. From this figure, it can be observed that larger variations of the rotation axes may lead to larger nonlinear errors. Therefore, in actual machining, higher accuracy can be achieved under the condition that larger variations of the rotation axes are avoided.

(3) Define the rotation incremental ratio $\boldsymbol{K_i}$ as $\triangle\theta_{k,i}/\triangle\theta_{m,i}$. If $\boldsymbol{K_i}$ is small enough, the influence of $\theta_{m,i}$ on the nonlinear error δ_{Ii} can be ignored and the corresponding nonlinear error can be estimated according to (26). Figure 6 shows that the range of variation of the nonlinear error increases when the rotation incremental ratio K_i varies from 1/2, 1, 2, to 3 under the conditions that $\triangle\theta_{m,i} \in [-\pi/9, \pi/9]$ and $\theta_{m,i} \in [-\pi, \pi]$.

(4) Under the condition that the incremental values of the two rotation axes $\Delta\theta_{k,i}$ and $\Delta\theta_{m,i}$ are fixed, the nonlinear error δ_{Ii} can be considered as a periodic function whose independent variable is $\theta_{m,i}$ and the minimum positive period is π. The symmetric line of the periodic function can be expressed as

$$\theta_{m,i} = \frac{N}{2}\pi - \frac{\Delta\theta_{m,i}}{2} \quad N = 0, \pm 1, \ldots, \pm n. \tag{27}$$

Figure 7 presents periodical variation of the nonlinear error when the rotation incremental ratio K_i varies from 1/2, 2, 3, to 5 under the conditions that $\triangle\theta_{m,i} = \pi/6$ and $\theta_{m,i} \in [-\pi, \pi]$. From this figure, it can be observed that the minimum positive period is π. It also can be observed that the symmetric lines are $\theta_{m,i} = -7\pi/12$, $\theta_{m,i} = -\pi/12$, $\theta_{m,i} = 5\pi/12$, and $\theta_{m,i} = 11\pi/12$.

4.2. General Formula and Common Rules of Nonlinear Error due to Rotation Movement for Machine Tools in Group II. In Section 4.1, the general formula of nonlinear error for machine tools in Group I was presented and the common rules were summarized. In this section, the general formula and common rules of nonlinear error for machine tools in Group II are analyzed. According to the equation for nonlinear error proposed in Section 3, the detailed expressions of $\alpha_{i,u}$ due to the rotational movement for different types of

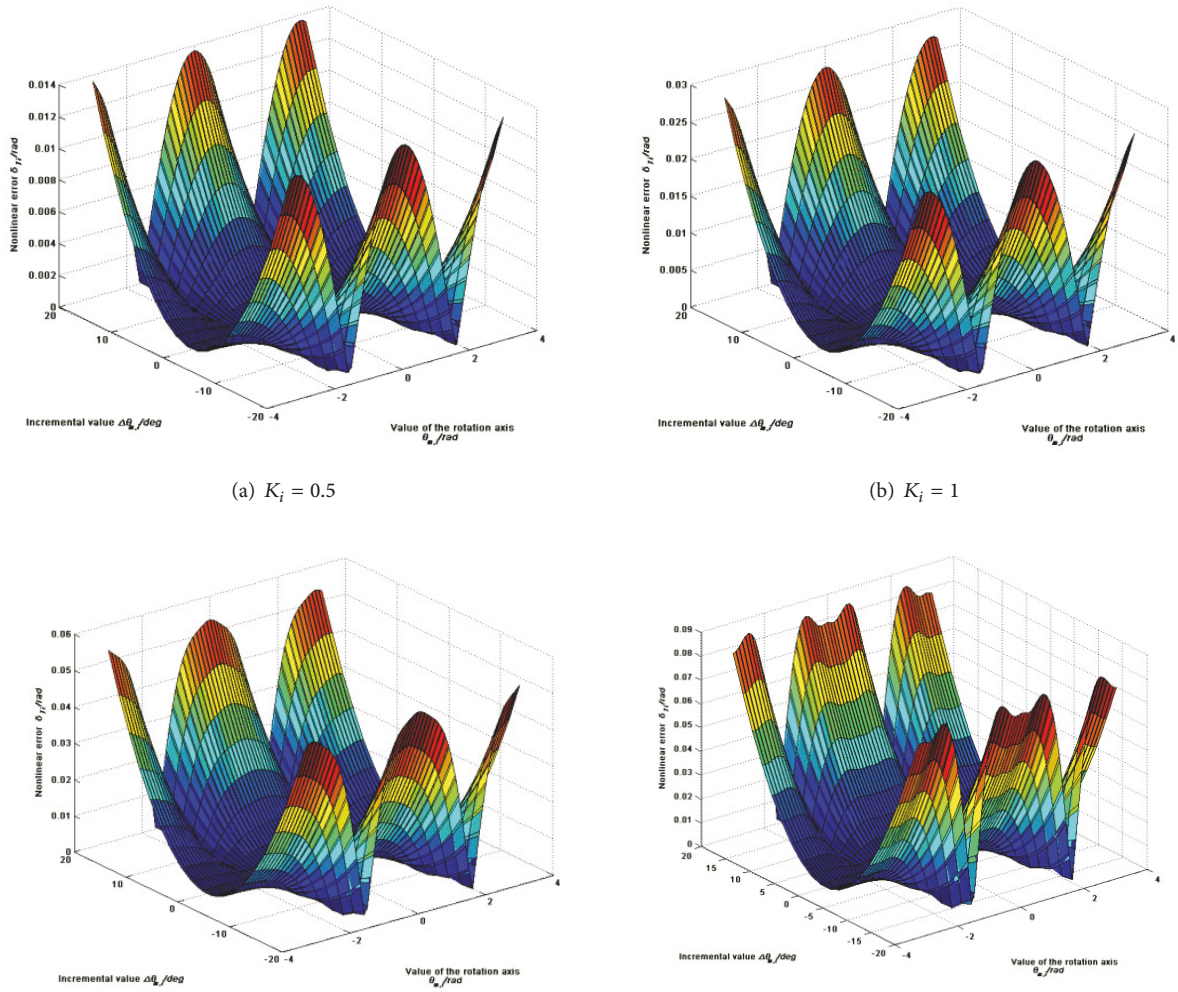

(a) $K_i = 0.5$ (b) $K_i = 1$

(c) $K_i = 2$ (d) $K_i = 3$

FIGURE 6: Influence of K_i on nonlinear error δ_{1i}.

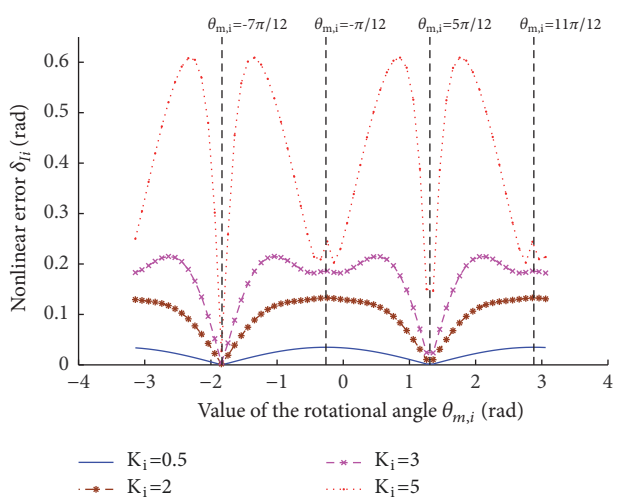

FIGURE 7: Periodical variation of nonlinear error when $\triangle\theta_{m,i} = \pi/6$.

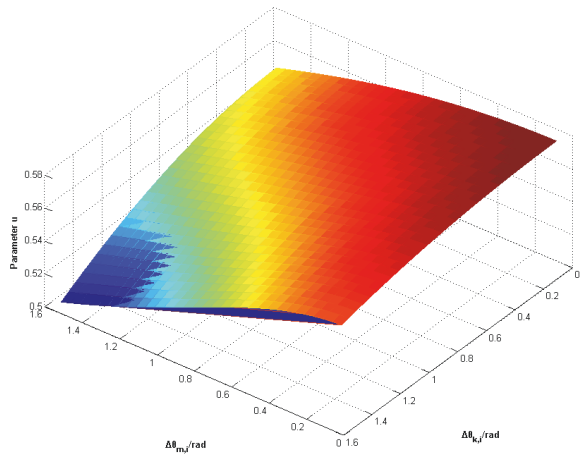

FIGURE 8: Parameter u corresponding to maximum $\alpha_{i,u}$ for machine tools in Group II.

machine tools in Group II are as presented in Table 3. The calculation procedure for the machine tool of type ABZ is taken as an example for the explanation in Appendix B and this procedure can also be extended to the other types in Group II.

From Table 3, it can be concluded that when the two rotary axes move from $\theta_{k,i}$ and $\theta_{m,i}$ to $\theta_{k,i+1}$ and $\theta_{m,i+1}$ respectively, the deviation of $S_{i,R}(u, 1)$ from the reference plane $S_{i,T}(u, 1)$ for machine tools in Group II can be expressed as

$$\alpha_{i,u} = \left| \frac{\cos(\theta_{m,i})\cos(\theta_{m,i+1})\sin((1-u)\theta_{m,i} + u\theta_{m,i+1})\sin(\theta_{k,i+1} - \theta_{k,i}) - \cos((1-u)\theta_{m,i} + u\theta_{m,i+1})\cos(\theta_{m,i+1})\sin(\theta_{m,i})\sin((1-u)(\theta_{k,i+1} - \theta_{k,i})) - \cos((1-u)\theta_{m,i} + u\theta_{m,i+1})\cos(\theta_{m,i})\sin(\theta_{m,i+1})\sin(u(\theta_{k,i+1} - \theta_{k,i}))}{\sqrt{1 - (\sin(\theta_{m,i})\sin(\theta_{m,i+1}) + \cos(\theta_{m,i})\cos(\theta_{m,i+1})\cos(\theta_{k,i+1} - \theta_{k,i}))^2}} \right| \quad (28)$$

where $\Delta\theta_{k,i}$ and $\Delta\theta_{m,i}$ are incremental values for the two rotation axes:

$$\begin{aligned} \Delta\theta_{k,i} &= \theta_{k,i+1} - \theta_{k,i} \\ \Delta\theta_{m,i} &= \theta_{m,i+1} - \theta_{m,i}. \end{aligned} \quad (29)$$

As is shown in Figure 8, the nonlinear error can be obtained under the condition that parameter u ranges between 0.5019 and 0.5773. For simplification, the value of $\alpha_{i,u}$ when u = 0.5 is used for the approximation of δ_{IIi}:

$$\delta_{IIi}(\theta_{m,i}, \Delta\theta_{m,i}, \Delta\theta_{k,i}) = \left| \frac{\cos(\theta_{m,i})\cos(\theta_{m,i} + \Delta\theta_{m,i})\sin(\theta_{m,i} + (1/2)\Delta\theta_{m,i})\sin(\Delta\theta_{k,i}) - \cos(\theta_{m,i} + (1/2)\Delta\theta_{m,i})\sin(2\theta_{m,i} + \Delta\theta_{m,i})\sin((1/2)\Delta\theta_{k,i})}{\sqrt{1 - (\sin(\theta_{m,i})\sin(\theta_{m,i} + \Delta\theta_{m,i}) + \cos(\theta_{m,i})\cos(\theta_{m,i} + \Delta\theta_{m,i})\cos(\Delta\theta_{k,i}))^2}} \right|. \quad (30)$$

Comparing (25) and (30), it can be observed that there exists a relationship of nonlinear errors due to motions of the rotation axes for machine tools in Group I and Group II:

$$\delta_{IIi}(\theta_{m,i}, \Delta\theta_{m,i}, \Delta\theta_{k,i}) = \delta_{Ii}\left(\frac{\pi}{2} + \theta_{m,i}, \Delta\theta_{m,i}, \Delta\theta_{k,i}\right). \quad (31)$$

Equation (31) indicates that the nonlinear error δ_{IIi} has properties that are similar to δ_{Ii}. Figure 9(a) depicts the nonlinear error due to the motions of the rotation axes for machine tools in Group I and Group II under the conditions that $\Delta\theta_{k,i} = 15^\circ$, $\Delta\theta_{m,i} = 30^\circ$, and $\theta_{k,i}$ varies from -2π to 2π. Similarly, Figure 9(b) shows the variation of the nonlinear error, while $\Delta\theta_{k,i} = 20^\circ$, $\Delta\theta_{m,i} = 60^\circ$, and $\theta_{k,i}$ varies from -2π to 2π.

5. Case Study

As shown in Figures 10(a), 10(b), and 10(c), CNC machine tools whose home positions are (0 0 1) and rotary axis features are AB and AC, respectively, are used for the machining of an impeller to further emphasize the practical aspects related to the issues we have discussed in previous sections.

Table 3: Detailed expressions of $\alpha_{i,u}$ for machine tools in Group II.

Type	Deviation of $S_{i,R}(u,1)$ from the reference plane $S_{i,T}(u,1)$
ABZ	$\left\lvert \frac{\cos(\theta_{Y,i})\cos(\theta_{Y,i+1})\sin((1-u)\theta_{Y,i}+u\theta_{Y,i+1})\sin(\theta_{X,i+1}-\theta_{X,i})-\cos((1-u)\theta_{Y,i}+u\theta_{Y,i+1})\cos(\theta_{Y,i+1})\sin(\theta_{Y,i})\sin((1-u)(\theta_{X,i+1}-\theta_{X,i}))-\cos((1-u)\theta_{Y,i}+u\theta_{Y,i+1})\cos(\theta_{Y,i})\sin(\theta_{Y,i+1})\sin(u(\theta_{X,i+1}-\theta_{X,i}))}{\sqrt{1-(\sin(\theta_{Y,i})\sin(\theta_{Y,i+1})+\cos(\theta_{Y,i})\cos(\theta_{Y,i+1})\cos(\theta_{X,i+1}-\theta_{X,i}))^2}} \right\rvert$
ACY	$\left\lvert \frac{\cos(\theta_{Z,i})\cos(\theta_{Z,i+1})\sin((1-u)\theta_{Z,i}+u\theta_{Z,i+1})\sin(\theta_{X,i+1}-\theta_{X,i})-\cos((1-u)\theta_{Z,i}+u\theta_{Z,i+1})\cos(\theta_{Z,i+1})\sin(\theta_{Z,i})\sin((1-u)(\theta_{X,i+1}-\theta_{X,i}))-\cos((1-u)\theta_{Z,i}+u\theta_{Z,i+1})\cos(\theta_{Z,i})\sin(\theta_{Z,i+1})\sin(u(\theta_{X,i+1}-\theta_{X,i}))}{\sqrt{1-(\sin(\theta_{Z,i})\sin(\theta_{Z,i+1})+\cos(\theta_{Z,i})\cos(\theta_{Z,i+1})\cos(\theta_{X,i+1}-\theta_{X,i}))^2}} \right\rvert$
BCX	$\left\lvert \frac{\cos(\theta_{Z,i})\cos(\theta_{Z,i+1})\sin((1-u)\theta_{Z,i}+u\theta_{Z,i+1})\sin(\theta_{Y,i+1}-\theta_{Y,i})-\cos((1-u)\theta_{Z,i}+u\theta_{Z,i+1})\cos(\theta_{Z,i+1})\sin(\theta_{Z,i})\sin((1-u)(\theta_{Y,i+1}-\theta_{Y,i}))-\cos((1-u)\theta_{Z,i}+u\theta_{Z,i+1})\cos(\theta_{Z,i})\sin(\theta_{Z,i+1})\sin(u(\theta_{Y,i+1}-\theta_{Y,i}))}{\sqrt{1-(\sin(\theta_{Z,i})\sin(\theta_{Z,i+1})+\cos(\theta_{Z,i})\cos(\theta_{Z,i+1})\cos(\theta_{Y,i+1}-\theta_{Y,i}))^2}} \right\rvert$
BAZ	$\left\lvert \frac{\cos(\theta_{X,i})\cos(\theta_{X,i+1})\sin((1-u)\theta_{X,i}+u\theta_{X,i+1})\sin(\theta_{Y,i+1}-\theta_{Y,i})-\cos((1-u)\theta_{X,i}+u\theta_{X,i+1})\cos(\theta_{X,i+1})\sin(\theta_{X,i})\sin((1-u)(\theta_{Y,i+1}-\theta_{Y,i}))-\cos((1-u)\theta_{X,i}+u\theta_{X,i+1})\cos(\theta_{X,i})\sin(\theta_{X,i+1})\sin(u(\theta_{Y,i+1}-\theta_{Y,i}))}{\sqrt{1-(\sin(\theta_{X,i})\sin(\theta_{X,i+1})+\cos(\theta_{X,i})\cos(\theta_{X,i+1})\cos(\theta_{Y,i+1}-\theta_{Y,i}))^2}} \right\rvert$
CAY	$\left\lvert \frac{\cos(\theta_{X,i})\cos(\theta_{X,i+1})\sin((1-u)\theta_{X,i}+u\theta_{X,i+1})\sin(\theta_{Z,i+1}-\theta_{Z,i})-\cos((1-u)\theta_{X,i}+u\theta_{X,i+1})\cos(\theta_{X,i+1})\sin(\theta_{X,i})\sin((1-u)(\theta_{Z,i+1}-\theta_{Z,i}))-\cos((1-u)\theta_{X,i}+u\theta_{X,i+1})\cos(\theta_{X,i})\sin(\theta_{X,i+1})\sin(u(\theta_{Z,i+1}-\theta_{Z,i}))}{\sqrt{1-(\sin(\theta_{X,i})\sin(\theta_{X,i+1})+\cos(\theta_{X,i})\cos(\theta_{X,i+1})\cos(\theta_{Z,i+1}-\theta_{Z,i}))^2}} \right\rvert$
CBX	$\left\lvert \frac{\cos(\theta_{Y,i})\cos(\theta_{Y,i+1})\sin((1-u)\theta_{Y,i}+u\theta_{Y,i+1})\sin(\theta_{Z,i+1}-\theta_{Z,i})-\cos((1-u)\theta_{Y,i}+u\theta_{Y,i+1})\cos(\theta_{Y,i+1})\sin(\theta_{Y,i})\sin((1-u)(\theta_{Z,i+1}-\theta_{Z,i}))-\cos((1-u)\theta_{Y,i}+u\theta_{Y,i+1})\cos(\theta_{Y,i})\sin(\theta_{Y,i+1})\sin(u(\theta_{Z,i+1}-\theta_{Z,i}))}{\sqrt{1-(\sin(\theta_{Y,i})\sin(\theta_{Y,i+1})+\cos(\theta_{Y,i})\cos(\theta_{Y,i+1})\cos(\theta_{Z,i+1}-\theta_{Z,i}))^2}} \right\rvert$

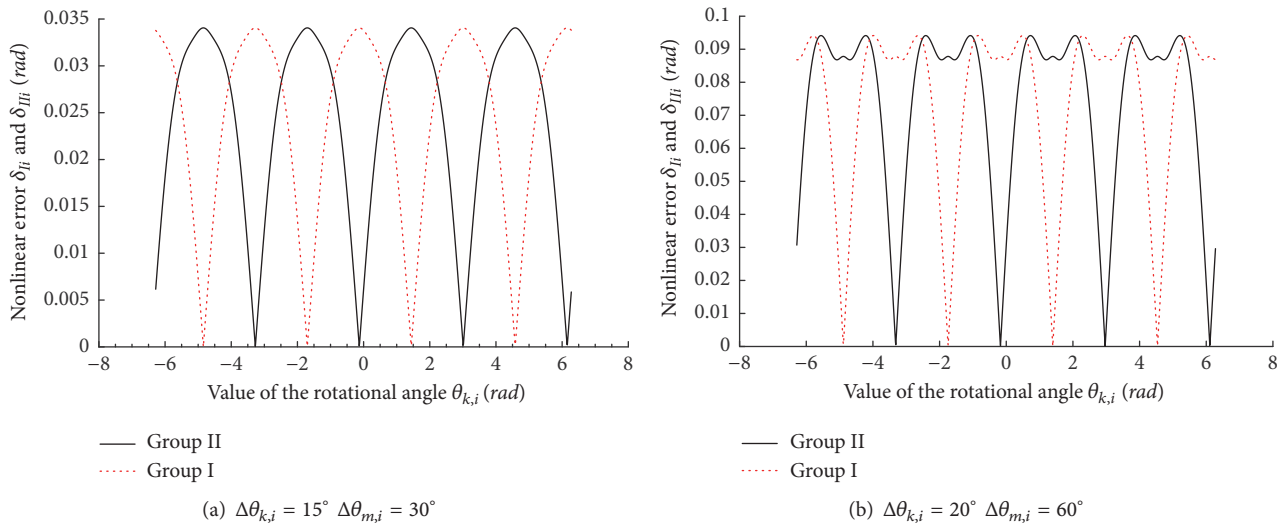

Figure 9: Comparison of nonlinear error for machine tools in Group I and Group II.

(a) (b) (c)

Figure 10: Machining conditions: (a) CNC machine tools whose home positions are $(0 \quad 0 \quad 1)$ and the rotary axis feature is AC; (b) CNC machine tools whose home positions are $(0 \quad 0 \quad 1)$ and rotary axis feature is AB; (c) impeller used for machining.

Considering the symmetry of the impeller, one path shown in Figure 11 is used for the simulation. As shown in Figure 12, while machining the same path using the two machine tools, the nonlinear errors due to the motions of the rotary axes are different. It can be further observed in Table 4 that the maximum nonlinear error varies from 0 rad to 0.0013 rad in the machining of the path for the AB machine. However, two abrupt areas exist in which the maximum nonlinear errors are 0.7181 rad and 0.8585 rad in the machining of the same path for the AC machine. Compared with the machine tool whose rotary axis feature is AC, higher accuracy can be achieved by using the machine tool whose rotary axis feature is AB. Therefore, the machine tool whose rotary axis feature is AB will be more suitable for the machining of the impeller.

Figure 13 reveals that a significantly smoother surface can be achieved in the machining of the impeller using machine tool whose rotary axis feature is AB, which agree with the conclusions from the simulation.

6. Conclusions

This study developed a general model to analyze the relationship between nonlinear errors and the movement of the rotation axes for various machine configurations. Although spline curves are widely used in modern five-axis CNC systems to avoid nonlinear errors caused by motion of the linear axes, little attempt has been made to obtain common rules for nonlinear errors due to motions of the rotation axes.

In this paper, five-axis CNC machine tools were classified into two groups according to the configuration of two rotational joints and the home position of the tool orientation. The motions of the tools were regarded as a combination of translation and rotation. The maximum deviation of the tool with respect to the reference plane generated by the initial and the final orientation were used to quantify the magnitude of the errors. General formulas were derived and common change rules were analyzed for machine tools in the two groups.

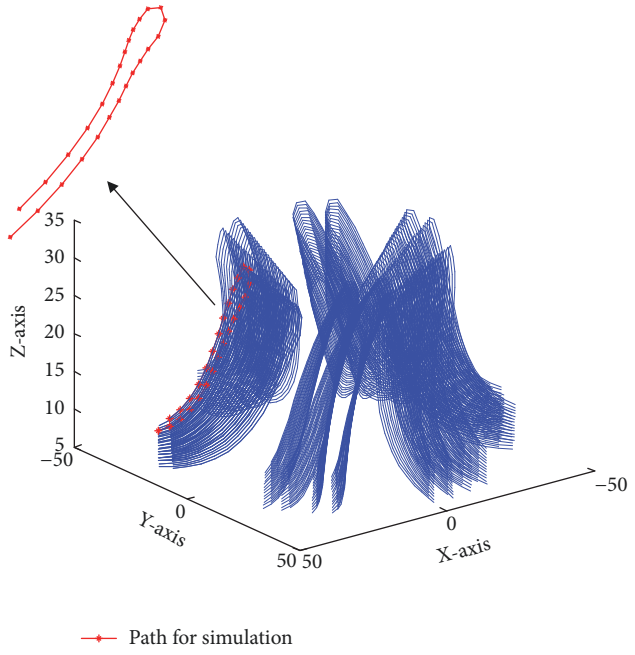

Figure 11: Tool path for simulation.

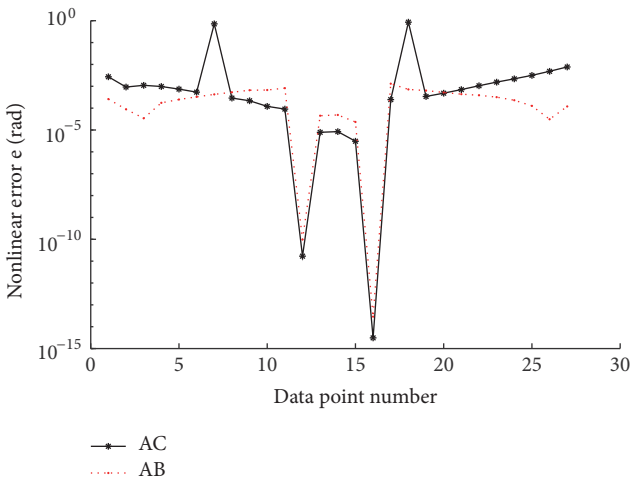

Figure 12: Nonlinear errors due to motions of rotary axes of the two machine tools.

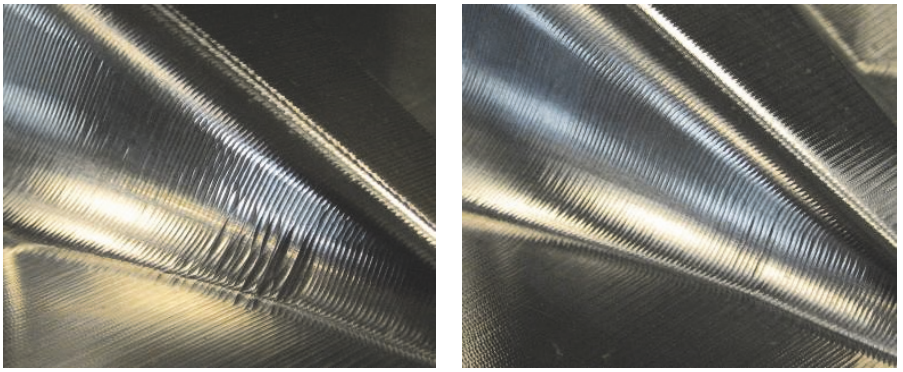

(a) (b)

Figure 13: Machining effects: (a) AC machine tool and (b) AB machine tool.

Table 4: Comparison of nonlinear errors for the same path with CNC machine tools whose rotary axis features are AB and AC.

Data point number	Nonlinear error for AB machine tool	Nonlinear error for AC machine tool
1	0.0003	0.0027
2	0.0001	0.0009
3	0.0000	0.0011
4	0.0002	0.0010
5	0.0002	0.0007
6	0.0003	0.0005
7	0.0004	0.7181
8	0.0005	0.0003
9	0.0007	0.0002
10	0.0007	0.0001
11	0.0008	0.0001
12	0.0000	0.0000
13	0.0000	0.0000
14	0.0000	0.0000
15	0.0000	0.0000
16	0.0000	0.0000
17	0.0013	0.0002
18	0.0007	0.8585
19	0.0006	0.0003
20	0.0005	0.0005
21	0.0004	0.0007
22	0.0004	0.0011
23	0.0003	0.0016
24	0.0002	0.0022
25	0.0001	0.0032
26	0.0000	0.0049
27	0.0001	0.0077

A comparison of the two general formulas obtained shows that relational expressions for nonlinear errors due to the motions of the rotary axes between both groups can be derived, which indicate the existence of similar properties described as follows. First, nonlinear error can be represented as a function with only the position of one rotation axis and incremental values of both rotation axes. Second, the amplitude of the nonlinear error increases with the incremental ratio. Third, if the rotation incremental ratio is small enough, the influence of the position of the rotation axes on the nonlinear error can be ignored. In this situation, the nonlinear error can be represented as a function that is only related to the variations of the two rotation axes. Moreover, under the condition that the incremental values of the two rotation axes are fixed, the nonlinear error can be considered as a periodic function.

In this paper, the linear interpolation method was used as an example under the consideration that this method is widely used in real machining. However, the same calculation model can be directly used and similar analysis can be carried out for other interpolation methods. This work gives an important future investigation direction that combines the analysis of nonlinear error due to the movement of rotation axes with kinematic configuration selection and tool path planning to improve the overall five-axis machining accuracy for a specific machining task. The limitation of this study lies in the fact that the axes of the machine are assumed to be orthogonal, which means that the conclusions obtained cannot be applied to five-axis machine tools with a nutating head whose rotational axis is in an inclined plane.

Appendix

A.

For machine tools whose rotary axis features are AB and home position is $(1\ \ 0\ \ 0)$, the tool orientations V_i and V_{i+1} corresponding to positions where the rotation angles are $(\theta_{X,i}, \theta_{Y,i})$ and $(\theta_{X,i+1}, \theta_{Y,i+1})$, respectively, can be expressed as

$$V_i = \begin{pmatrix} \cos\theta_{Y,i} \\ \sin\theta_{X,i} \cdot \sin\theta_{Y,i} \\ -\cos\theta_{X,i} \cdot \sin\theta_{Y,i} \end{pmatrix},$$
$$V_{i+1} = \begin{pmatrix} \cos\theta_{Y,i+1} \\ \sin\theta_{X,i+1} \cdot \sin\theta_{Y,i+1} \\ -\cos\theta_{X,i+1} \cdot \sin\theta_{Y,i+1} \end{pmatrix}. \tag{A.1}$$

When the tool orientation changes from V_i to V_{i+1}, $S_{i,R}(u, 1)$ can be expressed as

$$S_{i,R}(u,1) = \begin{pmatrix} \cos\theta_{Y,i}(u) \\ \sin\theta_{X,i}(u) \cdot \sin\theta_{Y,i}(u) \\ -\cos\theta_{X,i}(u) \cdot \sin\theta_{Y,i}(u) \end{pmatrix}, \tag{A.2}$$

where $\theta_{X,i}(u)$ and $\theta_{Y,i}(u)$ satisfy the following equations:

$$\theta_{X,i}(u) = (1-u)\,\theta_{X,i} + u\theta_{X,i+1}$$
$$\theta_{Y,i}(u) = (1-u)\,\theta_{Y,i} + u\theta_{Y,i+1}. \tag{A.3}$$

$S_{i,T}(u, 1)$ determined by V_i and V_{i+1} can be expressed as follows:

$$S_{i,T}(u,1) = \cos\phi_i(u)\,\mathbf{V}_i + \sin\phi_i(u)\,\frac{V_{i+1} - \cos\phi_i(1)\,V_i}{\sin\phi_i(1)}, \tag{A.4}$$

where $\varphi_i(u)$ is a function whose parameter is u:

$$\phi_i(u) = \arccos\left(\cos\theta_{Y,i+1} \cdot \cos\theta_{Y,i} + \sin\theta_{X,i+1} \cdot \sin\theta_{Y,i+1} \cdot \sin\theta_{X,i} \cdot \sin\theta_{Y,i} + \cos\theta_{X,i+1} \cdot \sin\theta_{Y,i+1} \cdot \cos\theta_{X,i} \cdot \sin\theta_{Y,i}\right) \cdot u. \tag{A.5}$$

Using MATLAB file ABX.m for evaluating the dot-product of $S_{i,R}(u, 1)$ and $S_{i,T}(u, 1)$, $\alpha_{i,u}$ can be expressed by using $\theta_{X,I}$, $\theta_{Y,I}$, $\theta_{X,i+1}$, and $\theta_{Y,i+1}$ as parameters:

$$\left|\frac{\sin(\theta_{Y,i})\sin(\theta_{Y,i+1})\cos((1-u)\theta_{Y,i}+u\theta_{Y,i+1})\sin(\theta_{X,i+1}-\theta_{X,i})-\sin((1-u)\theta_{Y,i}+u\theta_{Y,i+1})\sin(\theta_{Y,i+1})\cos(\theta_{Y,i})\sin((1-u)(\theta_{X,i+1}-\theta_{X,i}))-\sin((1-u)\theta_{Y,i}+u\theta_{Y,i+1})\cos(\theta_{Y,i+1})\sin(\theta_{Y,i})\sin(u(\theta_{X,i+1}-\theta_{X,i}))}{\sqrt{1-(\cos(\theta_{Y,i})\cos(\theta_{Y,i+1})+\sin(\theta_{Y,i})\sin(\theta_{Y,i+1})\cos(\theta_{X,i+1}-\theta_{X,i}))^2}}\right| \quad (A.6)$$

B.

For machine tools whose rotary axis features are AB and home position is $(0\ \ 0\ \ 1)$, the tool orientations V_i and V_{i+1} corresponding to positions where the rotation angles are $(\theta_{X,i}, \theta_{Y,i})$ and $(\theta_{X,i+1}, \theta_{Y,i+1})$, respectively, can be expressed as

$$V_i = \begin{pmatrix} \sin\theta_{Y,i} \\ -\sin\theta_{X,i}\cdot\cos\theta_{Y,i} \\ \cos\theta_{X,i}\cdot\cos\theta_{Y,i} \end{pmatrix}, \quad V_{i+1} = \begin{pmatrix} \sin\theta_{Y,i+1} \\ -\sin\theta_{X,i+1}\cdot\cos\theta_{Y,i+1} \\ \cos\theta_{X,i+1}\cdot\cos\theta_{Y,i+1} \end{pmatrix}. \quad (B.1)$$

When the tool orientation changes from V_i to V_{i+1}, $S_{i,R}(u,1)$ can be expressed as

$$S_{i,R}(u,1) = \begin{pmatrix} \sin\theta_{Y,i}(u) \\ -\sin\theta_{X,i}(u)\cdot\cos\theta_{Y,i}(u) \\ \cos\theta_{X,i}(u)\cdot\cos\theta_{Y,i}(u) \end{pmatrix}, \quad (B.2)$$

where $\theta_{X,i}(u)$ and $\theta_{Y,i}(u)$ satisfy the following equations:

$$\theta_{X,i}(u) = (1-u)\theta_{X,i} + u\theta_{X,i+1}$$

$$\theta_{Y,i}(u) = (1-u)\theta_{Y,i} + u\theta_{Y,i+1}. \quad (B.3)$$

$S_{i,T}(u,1)$ determined by V_i and V_{i+1} can be expressed as follows:

$$S_{i,T}(u,1) = \cos\phi_i(u)\,\mathbf{V}_i + \sin\phi_i(u)\,\frac{V_{i+1}-\cos\phi_i(1)\,V_i}{\sin\phi_i(1)}, \quad (B.4)$$

where $\varphi_i(u)$ is a function whose parameter is u:

$$\phi_i(u) = \arccos(\sin\theta_{Y,i+1}\cdot\sin\theta_{Y,i} + \sin\theta_{X,i+1}\cdot\cos\theta_{Y,i+1}\cdot\sin\theta_{X,i}\cdot\cos\theta_{Y,i} + \cos\theta_{X,i+1}\cdot\cos\theta_{Y,i+1}\cdot\cos\theta_{X,i}\cdot\cos\theta_{Y,i})\cdot u. \quad (B.5)$$

Using MATLAB file ABZ.m for evaluating the dot-product of $S_{i,R}(u,1)$ and $S_{i,T}(u,1)$, $\alpha_{i,u}$ can be expressed by using $\theta_{X,i}$, $\theta_{Y,i}$, $\theta_{X,i+1}$, and $\theta_{Y,i+1}$ as parameters:

$$\left|\frac{\cos(\theta_{y,i})\cos(\theta_{y,i+1})\sin((1-u)\theta_{y,i}+u\theta_{y,i+1})\sin(\theta_{x,i+1}-\theta_{x,i})-\cos((1-u)\theta_{y,i}+u\theta_{y,i+1})\cos(\theta_{y,i+1})\sin(\theta_{y,i})\sin((1-u)(\theta_{x,i+1}-\theta_{x,i}))-\cos((1-u)\theta_{y,i}+u\theta_{y,i+1})\cos(\theta_{y,i})\sin(\theta_{y,i+1})\sin(u(\theta_{x,i+1}-\theta_{x,i}))}{\sqrt{1-(\sin(\theta_{y,i})\sin(\theta_{y,i+1})+\cos(\theta_{y,i})\cos(\theta_{y,i+1})\cos(\theta_{x,i+1}-\theta_{x,i}))^2}}\right| \quad (B.6)$$

Data Availability

Data and codes for experiment can be found in supplementary materials offered with the document.

Conflicts of Interest

The authors declare no conflicts of interest.

Acknowledgments

This work is supported by the National Science and Technology Major Project (Grant no. 2013ZX04001-031), Research Project of Education Department of Liaoning Province (Grant no. L2015438), Open Fund of National-Local Joint Engineering Laboratory (Grant no. SJSC-2015-08), Discipline Content Education Project (no. XKHY2-27), and Postdoctoral Research Fund of Shenyang Jianzhu University (Grant no. SJZUBSH201612).

Supplementary Materials

MATLAB codes that can be used for drawing all the figures in the paper are provided as supplementary materials. *(Supplementary Materials)*

References

[1] Q. Cheng, C. Wu, P. Gu, W. Chang, and D. Xuan, "An analysis methodology for stochastic characteristic of volumetric error in multiaxis CNC machine tool," *Mathematical Problems in Engineering*, vol. 2013, Article ID 863283, 12 pages, 2013.

[2] H. Perez, E. Diez, J. d. Marquez, and A. Vizan, "Generic Mathematical Model for Efficient Milling Process Simulation," *Mathematical Problems in Engineering*, vol. 2015, pp. 1–10, 2015.

[3] G. Zhong, C. Wang, S. Yang, E. Zheng, and Y. Ge, "Position geometric error modeling, identification and compensation for large 5-axis machining center prototype," *The International Journal of Machine Tools and Manufacture*, vol. 89, pp. 142–150, 2015.

[4] R. J. Cripps, B. Cross, M. Hunt, and G. Mullineux, "Singularities in five-axis machining: Cause, effect and avoidance," *The International Journal of Machine Tools and Manufacture*, vol. 116, pp. 40–51, 2017.

[5] J. Yang and Y. Altintas, "A generalized on-line estimation and control of five-axis contouring errors of CNC machine tools," *The International Journal of Machine Tools and Manufacture*, vol. 88, pp. 9–23, 2015.

[6] S. Guo, D. Zhang, and Y. Xi, "Global Quantitative Sensitivity Analysis and Compensation of Geometric Errors of CNC Machine Tool," *Mathematical Problems in Engineering*, vol. 2016, pp. 1–12, 2016.

[7] S. Ding, X. Huang, C. Yu, and W. Wang, "Actual inverse kinematics for position-independent and position-dependent geometric error compensation of five-axis machine tools," *The International Journal of Machine Tools and Manufacture*, vol. 111, pp. 55–62, 2016.

[8] F.-C. Chen, "On the structural configuration synthesis and geometry of machining centres," *Proceedings of the Institution of Mechanical Engineers, Part C: Journal of Mechanical Engineering Science*, vol. 215, no. 6, pp. 641–652, 2001.

[9] S. Sakamoto and I. Inasaki, "Analysis of Generating Motion for Five-Axis Machining Centers," *TRANSACTIONS OF THE JAPAN SOCIETY OF MECHANICAL ENGINEERS Series C*, vol. 59, no. 561, pp. 1553–1559, 1993.

[10] H. Ishizawa, M. Hamada, and F. Tanaka, "Form shaping function model of five-axis machine tools-classification of five-axis machine tools based on form shaping functions," in *Proceedings of the Fifth Sapporo International Computer Graphics Symposium*, pp. 64–69, 1991.

[11] E. L. J. Bohez, "Five-axis milling machine tool kinematic chain design and analysis," *The International Journal of Machine Tools and Manufacture*, vol. 42, no. 4, pp. 505–520, 2002.

[12] Y. H. Jung, D. W. Lee, J. S. Kim, and H. S. Mok, "NC post-processor for 5-axis milling machine of table-rotating/tilting type," *Journal of Materials Processing Technology*, vol. 130-131, pp. 641–646, 2002.

[13] R. -. Lee and C. -. She, "Developing a postprocessor for three types of five-axis machine tools," *The International Journal of Advanced Manufacturing Technology*, vol. 13, no. 9, pp. 658–665, 1997.

[14] C. She and R. Lee, "A Postprocessor Based on the Kinematics Model for General Five-Axis Machine Tools," *Journal of Manufacturing Processes*, vol. 2, no. 2, pp. 131–141, 2000.

[15] O. R. Tutunea-Fatan and H.-Y. Feng, "Configuration analysis of five-axis machine tools using a generic kinematic model," *The International Journal of Machine Tools and Manufacture*, vol. 44, no. 11, pp. 1235–1243, 2004.

[16] C.-H. She and C.-C. Chang, "Design of a generic five-axis post-processor based on generalized kinematics model of machine tool," *The International Journal of Machine Tools and Manufacture*, vol. 47, no. 3-4, pp. 537–545, 2007.

[17] F. Y. Peng, J. Y. Ma, W. Wang, X. Y. Duan, P. P. Sun, and R. Yan, "Total differential methods based universal post processing algorithm considering geometric error for multi-axis NC machine tool," *The International Journal of Machine Tools and Manufacture*, vol. 70, pp. 53–62, 2013.

[18] X. Zhou, X. Liu, M. Li, Z. Wang, and X. Meng, "Post-processor development of a five-axis machine tool with optimization tool radius compensation," *The International Journal of Advanced Manufacturing Technology*, vol. 88, no. 5-8, pp. 1505–1522, 2017.

[19] J. Yang and Y. Altintas, "Generalized kinematics of five-axis serial machines with non-singular tool path generation," *The International Journal of Machine Tools and Manufacture*, vol. 75, pp. 119–132, 2013.

[20] Y.-R. Hwang and C.-S. Liang, "Cutting errors analysis for spindle-tilting type 5-axis NC machines," *The International Journal of Advanced Manufacturing Technology*, vol. 14, no. 6, pp. 399–405, 1998.

[21] G. Srijuntongsiri and S. S. Makhanov, "Optimisation of five-axis machining G-codes in the angular space," *International Journal of Production Research*, vol. 53, no. 11, pp. 3207–3227, 2015.

[22] C. Jun, K. Cha, and Y. Lee, "Optimizing tool orientations for 5-axis machining by configuration-space search method," *Computer-Aided Design*, vol. 35, no. 6, pp. 549–566, 2003.

[23] B. Sencer, Y. Altintas, and E. Croft, "Modeling and control of contouring errors for five-axis machine tools-Part I: Modeling," *Journal of Manufacturing Science and Engineering*, vol. 131, no. 3, pp. 0310061–0310068, 2009.

[24] O. R. Tutunea-Fatan and M. S. H. Bhuiya, "Comparing the kinematic efficiency of five-axis machine tool configurations through nonlinearity errors," *Computer-Aided Design*, vol. 43, no. 9, pp. 1163–1172, 2011.

[25] X. Yang, Y. Zhou, Z. Chen, and F. Wang, "Analysis and control of tool path interpolation error in rotary axes motions of five-axis CNC milling," *Jixie Gongcheng Xuebao/Journal of Mechanical Engineering*, vol. 48, no. 3, pp. 140–146, 2012.

[26] C. Geng, D. Yu, L. Zheng, and H. Zhang, "Algorithm of optimization of rotation axes in free-form surface machining," *Jixie Gongcheng Xuebao/Journal of Mechanical Engineering*, vol. 48, no. 23, pp. 127–134, 2012.

[27] C. Geng, D. Yu, L. Zheng, H. Zhang, and F. Wang, "A tool path correction and compression algorithm for five-axis CNC machining," *Journal of Systems Science and Complexity*, vol. 26, no. 5, pp. 799–816, 2013.